Active thermography setup updating for NDE: a comparative study of regression techniques and optimisation routines with high contrast parameter influences for thermal problems — Source link ⧉

J. Peeters, Ebrahim Louarroudi, Boris Bogaerts, Seppe Sels ...+3 more authors

Institutions: University of Antwerp, Vrije Universiteit Brussel

Related papers:

- Model-reduction techniques for Bayesian finite element model updating using dynamic response data

- FE model updating based on hybrid genetic algorithm and its verification on numerical bridge model

- Benchmarking Optimisation Methods for Model Selection and Parameter Estimation of Nonlinear Systems

- Development of efficient model updating technique using multi-stage response surfaces and derringer's function

- On an algorithm for combined system optimisation and parameter estimation

Active thermography setup updating for NDE : a comparative study of regression techniques and optimisation routines with high contrast parameter influences for thermal problems

Active thermography setup updating for NDE:
a comparative study of regression techniques & optimisation routines with high contrast parameter influences for thermal problems

J. Peeters[a,*], E. Louarroudi[a], B. Bogaerts[a], S. Sels[a], J.J.J. Dirckx[b], G. Steenackers[a,c]

[a]*University of Antwerp, Op3Mech research group, Faculty of Applied Engineering, Groenenborgerlaan 171, B-2020 Antwerp, Belgium. Tel.: +32-3-2051938*
[b]*University of Antwerp, Laboratory of Biomedical Physics, Groenenborgerlaan 171, B-2020 Antwerp, Belgium.*
[c]*Vrije Universiteit Brussel, Acoustics & Vibration Research Group, Pleinlaan 2, B-1050, Brussels, Belgium.*

Abstract

An implementation of updating techniques similar to finite element updating in structural dynamics is developed for thermal material inspection using adaptive response surfaces to approximate experimental parameters. In general, thermal models contain high non-linearities in their parameters which influences updating accuracies. This is further investigated in this work. Several adaptive response surface regression methods are compared: interpolation, piecewise spline and polynomial regression functions. Next, the influence of the choice of optimisation parameters is discussed and compared with several global and local optimisation routines. Finally, a well-suited regression technique is investigated which transforms the dataset to a smaller, focused response model in each optimisation loop and delivers a proper regression accuracy. This results in data-reduction for the model to be optimised.

Keywords: Pulsed Thermography, FE model updating (FEMU), Gradient based Optimisation, Genetic Optimisation, Inverse Problem, Simplex Method, evolutionary Strategy, Nondestructive Evaluation

*Ing. Jeroen Peeters
Email address: `jeroen.peeters2@uantwerpen.be` (J. Peeters)
URL: `www.op3mech.be` (J. Peeters)

1. Introduction

Computer simulation is an economic and quick way to determine and simulate material behaviour. The use of Finite element analysis (FEA) in the design of large structures is exponentially growing, but in uttermost cases the use of FEA remains in the design stage. Two of the largest drawbacks of the use of FEA beyond the design stage are the approximated material property parameters and the high computational cost to build an accurate FE model of the full structure. Finite element model updating (FEMU) could deliver a solution for these two disadvantages by updating with non-destructive testing data. These methods are widely used in modal vibration inspection [1–5], but their use is limited in thermal conductivity optimisation problems for problems with non-linear convection and radiation boundaries [6]. Inverse methods for the first-order partial differential equation (PDE) of the standard heat transfer problem containing conduction is described in details in [7]. The inverse problem of heat transfer functions with different mixed-boundary constrains are challenging to implement in FEMU routines due to the lack of an explicit relation between the model and the experimental measurements. Furthermore, after production of the structure, there is often no link between the material properties in the FE model and the real material characteristics. The FE models can be updated to the real state of the structure with a properly defined FEMU strategy based on an optimisation method.

FEA has been applied as a verification tool in a number of applications involving infrared thermography for Non-destructive evaluation (NDE) applications [8–11], but the use of FEMU on thermal radiation for active thermography is relatively original. There are a few differences with well-known modal optimisation for the reasons that the physical equation is a first order partial differential equation and that thermal modes are described differently from vibration modes [12]. This results in a different manner of defining the objective function and solver choice described in Section 3.3. Besides, an extreme non-linear behaviour of the response to limited parameter differences and a large dependency on the absolute temperature of the parameter influence are common in thermal FEMU but rare in structural dynamics.

Thermography is a growing evaluation technique and has become a widely used NDE technique for damage detection in metallic structural elements [13], as well as CFRP (Carbon fiber reinforced polymer) and GFRP (Glass fiber reinforced polymer) composites [14]. Especially with the increasing application of composite laminates such as CFRPs and GFRPs, the thermal conductances inside the components becomes anisotropic and quantitative prediction becomes complex. The generally used form of active thermography makes use of heat pulses emitted to the surfaces and is called Pulsed thermography (PT) [15]. There are countless advantages of thermography, these include the fact that it is a non-contact inspection and measurement technique, it can be performed in-situ, it can cover large areas and it is a quantitative method [16]. The problem of signal processing is essential in the field of active thermography. With the assistance of dedicated developed image and signal processing algorithms, it is possible to detect minuscule (μm) discontinuities inside structures. By reducing the amount of data and optimising the experimental setup, the process is speeded up, but a certain decrease in accuracy has to be kept in mind.

In this paper, the best optimisation strategy is searched based on the adaptive response surface method developed for modal analysis of a vibration problem in [17]. Due to the different parameter

behaviour in the thermal models, the best FEMU methodology will differ from the one in structural dynamics as compared in [18]. In this paper, a robust, efficient method is searched to build an accurate FE model by using FEMU with reduced PT data. Therefore, a comparison is made between different optimisation strategies modified from structural dynamics FEMU methods to compare the behaviour with literature on Structural Dynamics. In order to reduce the optimisation time, the method developed by Peeters et al. of [19] makes use of a regression model. Within this work, at both the level of regression model and the level of optimisation strategy, a comparison will be made with modified state-of-the-art techniques meant for structural dynamics to further improve the results in [19]. The three utmost used regression methods in recent literature are n-dimensional piecewise spline models, piecewise polynomial models and n-dimensional linear interpolation. Most of these techniques are used in vision applications or statistical modelling instead of FEMU routines [20, 21]. As the use of machine learning techniques like neural networks needs a large training step which should be repeated for each FE iteration in the analysis, this method is not included in the comparison [18, 22, 23]. Not all optimisation routines are applicable for FEMU due to the limited amount of initial points in the design space [5]. The selection of the tested optimisation methods is based on the results of the comparison in [18] for structural dynamics. A comparison is made between the best gradient-based method of [19] (a least-squared non-linear curve fitting algorithm based on the trust-region method) and three non-gradient based methods: a Nelder-Mead simplex method, a particle swarm evolutionary optimization method and a genetic algorithm as shown in [18] to be promising techniques for FEMU.

The paper is organised starting with a description of the test case, containing the experimental measurements and the definition of the FE model in Comsol Multiphysics 5.0. Afterwards, the optimisation method based on an adaptive response surface method, described in [19] is adapted and the influence of the chosen parameters is discussed. A comparison is made between different response surface fitting techniques, for all the FE mesh points. These response surfaces are used with multiple optimisation solvers and several broadly used optimisation algorithms. The results are verified using a sensitivity analysis and a uniqueness study. Finally, the modification of the experimental parameters of the FE model to the realistic values of the test sample are feasible.

2. Description of the test case

In section 3, the optimisation routine is described based on a specific thermographic experiment, widely used for validation of modern PT NDE algorithms. The goal is to retrieve an FE model with the same thermal response as measured with the experimental validation.

2.1. Experimental measurements

Test sample. Flat bottom hole plates are widely used to simulate the temperature impedance of delamination failures in composite materials. In this research, the used material is a homogeneous Poly vinyl chloride (PVC) test plate where it is impossible to retrieve by accident unforeseen delamination failures. The chosen test case delivers a bypass methodology for false positive measurements. In this study, the behaviour of the material properties of the test plate is approximated as being isotropic [24].
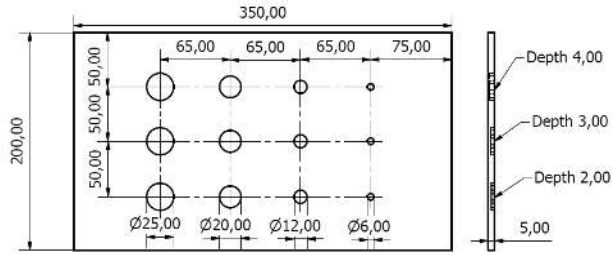
3

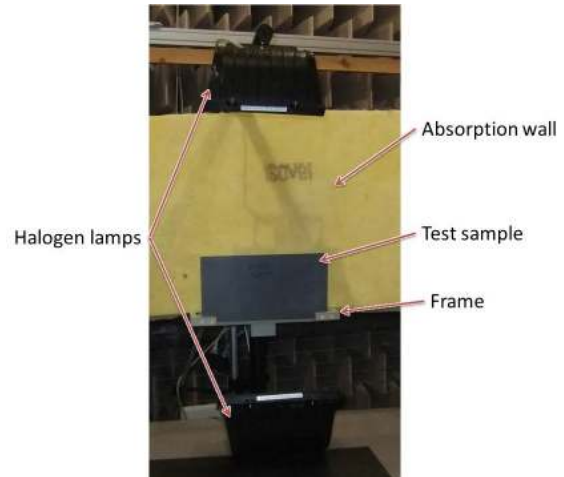Figure 1: Technical drawing of the Flat Bottom Hole plate.

Figure 2: Experimental setup in an anechoic chamber.

Experimental setup. The PVC plate as shown in Figures 1 and 2 is heated by two heat sources of 1 000 W electrical power each orientated to the test plate. The sources are positioned straight to the plate as shown in Figure 2. A Xenics Gobi 640 microbolometer camera is used with a detector wavelength range of 8-14 μm, a Noise equivalent temperature difference (NETD) of $\leq$ 50mK and a frame size of 640x480 pixels [25, 26]. The camera is placed on the centre-to-centre distance between both heat sources as shown in Figure 2. The heating stage is a 1 sec flash heating and the cooling is monitored for 100 seconds. The camera and heat sources are located at a distance of 1 m. The atmospheric conditions are held stable and the measurements are performed in a climatically isolated environment. The dimensions of the test sample and the sizes of the flaws inside the PVC test sample are shown in Figure 1. The experimental measurements are used to update the initial verification model with respect to the method described by [19] and further explained in Section 3.

Fundamentals of Pulsed Thermography. The PT measurements are used to validate the optimisation routines. This active-thermography NDE technique is based on the response analysis of the surface temperature of the structure to an emitted thermal wave initiated by an excitation pulse [27]. In this study, the reflective mode [11] is used whereby defective areas appear with a local higher temperature related to the thermal diffusivity of the defect. The thermal data are stored for several time steps which delivers a 3D matrix with in the XY-direction the temperature of each pixel and in the Z-direction each time frame [11, 28]. Local material properties, thickness or experimental setup parameters such as excitation power and distance can be defined [11]. The measurement accuracies are dependent on the ambient parameters: ambient temperature, emissivity, reflecting temperature and humidity. These parameters should be included in the optimisation routine if they are not controllable. The accuracy of the thermography measurement can be increased by image processing of the data using PPT (Pulsed phase thermography), or by other methods described in [11, 27, 29].
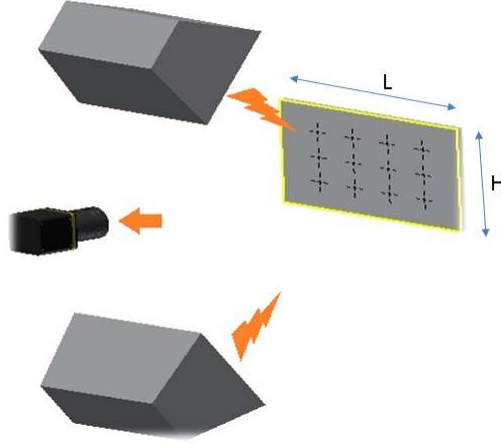
Figure 3: Schematic view of the experimental setup with the PVC plate

2.2. FE model

The model is built and simulated in the commercial FE multiphysics software COMSOL Multiphysics 5.2 and a constant, Newtonian non-linear method is used with a modernised implementation of the Differential algebraic equation (DAE) solver which uses backwards differentiation formulas [30]. There is made use of 2940 triangular linear Lagrange elements with a maximal growth rate of 1.3. To simulate the time dependent heat radiation from an external source to the inspected surface and the emitted response of the surface [31]. A schematic representation of the simulated model is shown in Figure 3. The centres of the defects, projected on the sample surface are the evaluated points for the comparison between experimental validation and the numerical model. It should be noted that the experiments and FE model are similar to those in [19], but for convenience of the reader the setting is repeated in the following section.

Governing Physics.

$$\rho C_p \frac{\partial T}{\partial t} + \nabla.(-\kappa \nabla T) = Q \text{ with } T(x,y,z,0) = T_\infty = 292.88\,[K] \tag{1}$$

The governing differential equation is a conductive heat transfer with an external heat source, formulated in Eq. (1) where ρ is the density, C_p is the material heat capacity at constant pressure, T is the absolute surface temperature in Kelvin, κ is the material thermal conductivity, t is the time and $Q(t)$ is the time-dependent heat source [28, 32]. The air between the lamps and the surface is neglected. Nearly all boundary conditions are defined according to reference [12, 31] only the boundary condition of the front and back surfaces should receive special attention. The boundary condition of the front (and back) surface:

$$-\kappa \frac{\partial T}{\partial x} = -\kappa \frac{\partial T}{\partial y} = h(T - T_\infty) + \sigma \varepsilon \left(T^4 - T_\infty^4\right); \ t > 0; \ 0 < x < H; \ 0 < y < L; \tag{2}$$

5

Table 1: Material Properties [40, 41].

	PVC
Heat source power P [W]	1000
Heat Capacity C_p $[J/(Kg.K)]$	1050
Density ρ $[Kg/m^3]$	1445
Surface Emissivity	0.92

The depth of an occurring defect can be found using the known diffusion length μ as widely validated in [33–36], which can be estimated from the following equation:

$$z = C_1 \sqrt{\frac{\alpha}{\pi \cdot f_b}} = C_1 \cdot \mu \text{ with } \alpha = \kappa/C_p\rho \tag{3}$$

Here α is the thermal diffusivity, L, H and d are respectively the length, the height and thickness of the plate in (m), h is the convective heat transfer coefficient, σ is the Stephan-Boltzmann constant, f_b the blind frequency, C_1 a constant typically equal to 1.82 [33] and ε is the emissivity in function of θ, the angle between the ray and the normal vector as defined in [37]. The convective heat transfer coefficient is calculated according to [38] from the knowledge that it is a vertical plate considering natural convection with a vertical length of the plate equal to H. The ambient temperature T_∞ equals 292.88 K. The numerical solution can be considered sufficiently accurate for thermographic NDE applications as described in [39].

$$Q(t) = \varepsilon \left(P(t) + F_\infty \sigma T_\infty^4 - \sigma T^4 \right) + h \cdot (T_\infty - T) \text{ with } \begin{cases} P(t) = P & for\, t \leq 5 \\ P(t) = 0 & for\, t > 5 \end{cases} \tag{4}$$

The external heat source has a non-linear characteristic as defined in Eq. (4) where, F_∞ is the field of view factor of the ambient reflections, and P is the power of the heat source [32]. A few simplifications are made:

- The air velocity is assumed to be 0 (due to the laboratory characteristics).

- The thermal conductivity κ of PVC is isotropic [24].

- The test sample is opaque and behaves equal to an ideal grey body which makes ε independent of θ [37].

The fixed parameters of the numerical model, which are not used within the optimisation routine, are described in Table 1. The field of view factor is computed automatically within the numerical simulation software [31].

3. Methodology

The developed optimisation routine makes use of an adaptive response surface regression to use a limited initial amount of FE models to feed an optimisation routine which is specifically

6

designed for general thermal problems where parameters linked to the general heat equation can be optimised or estimated using experimental input data. The algorithm uses a pan and zoom function to move through the design space and delivers faster predictions with fewer iterations than standard updating routines [17, 19].

3.1. Adaptive response surface method (ARSM)

The adaptive response surface optimisation routine is used to optimise numerical models with lots of data points and the time reducing by the algorithm increases as the number of parameters rises [5]. The ARSM methodology is initially mentioned by G. Wang [42] and simultaneously further developed by multiple researchers [5, 43–48]. The routine is designed to handle multiple-output time series data [19]. The optimisation procedure can be divided into the following steps and is shown schematically in Figure 4:

1. Starting reference simulation points is running and a correct objective function is built of the difference between the FE model and the target value (experiment or validation model).
2. The FE model is replaced by a meta-model of response surfaces.
3. The optimisation routine is run on a specific objective function.
4. The estimated parameter values are used as input parameters for an improved FE model that corrects the response model.
5. Only the points closer to the minimum are used to form the response surface.

As a benefit of step two, the optimisation time decreases without making the model less accurate. It is possible to use multiple objective functions or build an objective function related to multiple outputs within the third step. The main algorithm is originally published in [19], further details are repeated for convenience of the reader.

The response model which is optimised is not built from a pre-defined number of design experiments, but is adapted and refined during the optimisation routine by the pan and zoom command [19]. The method automatically calculates the parameter influence sensitivity and sequentially resolves multiple sets with first the major influencing parameters with fixed parameter values for the minor influencing parameters. Succeeding, the second parameter set is optimised and finally an influence check is performed for all parameter sets until the results converge. The selected optimisation parameters for this comparison are chosen to provide a heterogeneous parameter set with different non-linear response sensitivities across the time steps. The parameter set, symbolised by vector ϑ, is defined by:

- Pulse start time T_{pulse}(sec), which has major influences on the first 10 time steps and controls the amount of heat energy exposed to the test sample.

- Convective heat transfer coefficient h(W/m^{2}K), whose influences increases over time and is dependent on the temperature difference between the test sample and the ambient, making the parameter time dependent and implicitly related to the first parameter.

- Thermal conductivity k(W/m·K), which has a major impact on the heat distribution over time and is related to both the general PDE as shown in Eq.1 as to the boundary conditions as shown in Eq.2.
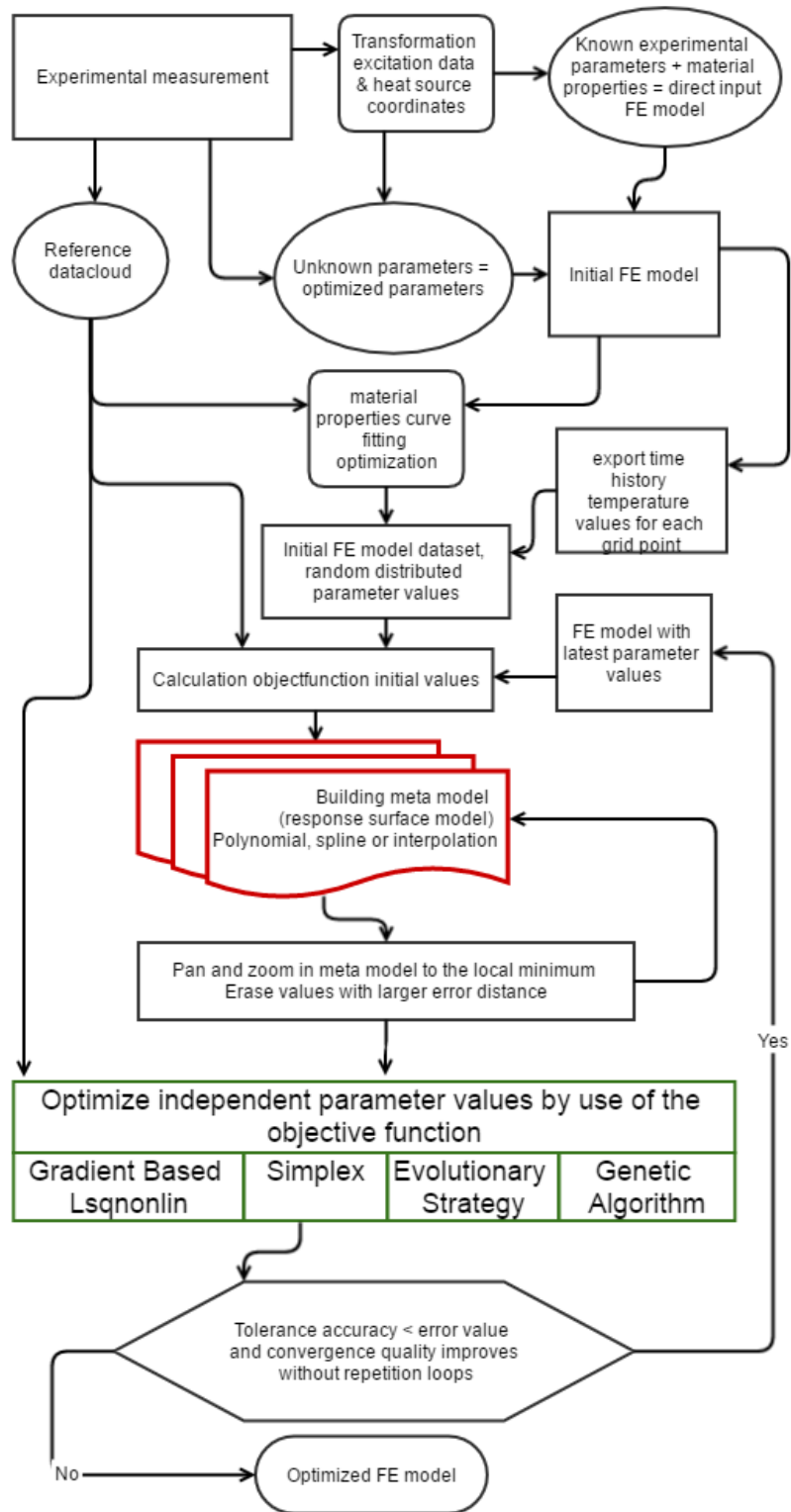
7

Figure 4: Schematical overview of the adaptive response surface optimisation routine.

The presence of a defect can be found by a local decrease of the thermal conductivity k with respect to the global parameter evaluation. As this manuscript is intended to compare the different optimisation solvers and regression techniques, only a global set of parameters is chosen. The objective function is defined identical for all optimisation solvers and response surface alternatives to deliver an objective comparison. The objective function is described in Eq.5 and consists of the difference between numerical estimated temperature and experimental temperature for all compared points distributed over the test sample.

$$\ell(\vartheta) = T_{model}(\vartheta) - T_{Ex} \tag{5}$$

3.2. Response surface alternatives

In this paper a comparison is made between three different response surface strategies in the time domain: a polynomial fitting, a scattered linear interpolation and a piecewise spline fitting, based on the ARESlab toolbox from [49].

Piecewise polynomial approximation. The first used regression technique is a multidimensional piecewise polynomial fitting, based on [17]. For all time steps, a regressive second-order polynomial model is made of the relative temperature on each time step versus the different optimisation parameters. This results in an $n + m$-dimensional response surface where n is the number of parameters and m the amount of time steps. This regression method delivers fast to evaluate response surfaces which have an overall accurate value for which it is mostly used for structural dynamics FEMU [17]. Major drawbacks are that the function value is non-local, which results in a sensitivity to approximations far from the specific function value and that it is an approximate method where the functions won't pass through the evaluation points itself [17, 42].

N-dimensional scattered linear interpolation. The second tested regression technique is a multi-dimensional linear interpolation of scattered data using the previous performed FE simulations within the design space [50]. A significant advantage is an exact fit of the data to the evaluation points and the fast local evaluation process. The drawback to linear behaviour can be that the global minimum is missed if a strong local minimum is already found before [51].

N-dimensional spline approximation. In this paper use is made of a piecewise least-squares spline fitting, based on the ARESlab toolbox from [49]. For every time step, a regressive spline model is made of the mean temperature of the plate surface versus the different optimisation parameters. It is ensured that the fit exactly goes through all evaluation points and a mix between linear, second-order and third-order polynomials is made between automatically defined control points. The changing of the number of control points is a drawback [51]. If the amount of control points remains fixed, the fit cannot be made optimal for all iterations. If the amount of control points changes through the iterations the multiple output accuracies are reduced and this reduces the speed of the method.

3.3. Optimisation solver

Four different optimisation solvers are used. The first one is a gradient-based non-linear least squares solver, specially adapted for curve fitting with multiple outputs (lsqcurvefit) [19, 51].

Table 2: Parameter boundary conditions [24, 40].

	Lower bound (lb)	Upper bound (ub)
Pulse start time T_{pulse} (sec)	0	2
Convective heat transfer coefficient h ($W/m^2 \cdot K$)	1	20
Thermal Conductivity κ ($W/m \cdot K$)	0.3	1.5

The other three are nongradient-based methods, described in [18] as best suitable for FE model updating in structural dynamics: The Nelder-Mead Simplex method, a particle-swarm evolutionary strategy and a genetic algorithm. All solvers are adapted to respect boundary values as shown in Table 2.

Gradient based non-linear least square curve fitting. The gradient-based optimiser is designed for non-linear, continuous problems with a continuous first derivative and is chosen for its stability and robust objective function adaptation and excellent results as shown in [19].

The first optimisation routine is an adaptation of the well-known non-linear least-squares strategy specially designed for curve fitting problems [51], defined in Eq.(6), where lb and ub are respectively the lower and upper bound of the parameter set ϑ and the summation is performed over all spatial points X and all time steps t until t_{end}. Hereby the objective function delivers predictions of the temperature values instead of the error function as described in Eq.(5).

$$\underset{\vartheta}{argmin} \sum_{t=0}^{t_{end}} \sum_{i=1}^{X} (T_{FE,i}(\vartheta,t) - T_{Ex,i})^2 \ with \ lb \leqslant \vartheta \leqslant ub \tag{6}$$

Within this optimiser, the Trust-region-reflective algorithm is used, based on the Gauss-Newton method. The Trust-region-reflective is especially adapted for the use of bound constraints and gave superior results than the Levenberg-Marquardt algorithm. Further information about the algorithms can be found in [51–54].

Simplex. The Nelder-Mead Simplex method is a non-gradient-based optimisation routine intentionally developed to optimise unconstrained optimisation problems using non-linear function evaluations [18]. It is known for its robust optimisation for low-dimensional global optimisation problems [55]. The basic Simplex algorithm is adapted for improved optimisation of constrained problems [56]. The gradient is numerical approximated by a bounded version of:

$$\ell_i(\vartheta,t) = \ell_0(\vartheta,t) + \frac{a}{n\sqrt{2}} \cdot \left(\sqrt{n+1} + n - 1\right) \cdot e_i + \sum_{k=1 \neq i}^{n} \left[\frac{a}{n\sqrt{2}} \cdot \left(\sqrt{n+1} - 1\right)\right] \cdot e_k \ with \ i = 1, n \tag{7}$$

where e is the unit base vector and the simplex dimension a is initiated around the initial value of the objective function ℓ.

According to [18], the convergence is measured using the following inequality:

$$\sqrt{\sum_{i=1}^{n+1} \frac{\left(f_i - \bar{f}\right)^2}{n}} < \tau \ with \ \bar{f} = \frac{1}{n+1} \sum_{i=1}^{n+1} f_i \tag{8}$$

10

where τ is a small positive scalar, computed using $\bar{f}$. Drawbacks are the lack of precise convergence theory, many iterations with insignificant improvement before convergence and numerical failure can occur for even smooth functions [18]. The main advantages are [18]:

- Major progress occurs in the initial iterations, which gives rapidly acceptable results;

- A single or double function evaluation is involved in each iteration, separately from a shrink transformation;

- An excellent decrease in function value results by using comparatively less function evaluations;

- Simplicity to interpret.

In this way, it is less expensive in terms of function calls than an expensive n-dimensional search [55].

Evolutionary strategy. The particle swarm evolutionary strategy is inspired by the model of flocking behaviour seen by birds [18]. The algorithm has a few major advantages such as automatic handling of variables scaling and the global search character [18]. The major disadvantage can be the premature convergence [18]. The covariance matrix adaptation version (CMA-ES) used in this manuscript is seen as one of the strongest updating routines for FEMU of single and multi-objective problems in structural dynamics [57]. This algorithm has the advantage to self-adapt the mutation distribution which makes the algorithm invariant against order-preserving transformations of the fitness function value [57]. The method should be able to give superior and sturdier results than the Simplex method as the amount of function evaluations raises far above $30 \cdot N$ where the algorithm is specially designed for [58]. The used implementation is originally described in [58].

Genetic algorithm. A Genetic algorithm optimisation routine is a widely used probabilistic optimisation technique, inspired by the natural evolution theory of Darwin where the survival of the fittest theory is applied to populations to optimise a function [18]. The speed of convergence is the main drawback of the method. In contrary, the significant advantages are the high probability of global minimum detection and the ability to fit non-smooth objective functions. As the heat pulse is discrete in nature by turning the source on and off, the temperature distribution over time has a non-smooth time step where the heat source is switched off. We have chosen to perform grey encoding to avoid fictive boundaries between consecutive values [59]. For further specific information on the implementation is referred to the specific literature: [51, 59–61].

3.4. Uniqueness & Sensitivity

The uniqueness of the optimisation routines is checked by performing an ill-possedness analysis. A global minimum of the objective function can be found and results in a unique solution in the region specified by the parameter limits. The stability of the convergence of the optimisation solutions is difficult to prove. Using the ARSM method as defined in section 3.1, a global solution of the results is achieved by starting from the four different corners of the initial central composite

design together with the central coordinate of the parameter set, built from the parameter boundary values as shown in Table 2. If at least three of the initial starting points deliver the same result, it is used further in the optimisation routine [19].

By Peeters et al. in [19], a simulation validation is performed to investigate if for a known parameter set the found result converge to the same parameter set by using a simulation target model. Due to the use of an heuristic methodology and the missing exact analytical solution, to the authors their knowledge it is not possible to better validate the stability of the solution. The sensitivity of the problem on the different parameters is investigated for all different regression models and optimisation solvers using a global and local sensitivity for each parameter as described by Cannavo in [62]. The global sensitivity has been found for all equal to 1, which means that the global answer is only sensitive to the parameters which are implemented in the optimisation routine. The sensitivity for each parameter is computed using the first order sensitivity coefficients based on the FAST (Fourier amplitude sensitivity test) methodology described by Cukier et al. [63]. The results of the FAST sensitivity analysis are provided in section 4.3.

4. Results

The results section first gives an overview within each regression technique of the performance of the different optimisation solvers in section 4.1. The number of iterations, iteration time and accuracy are evaluated by comparing it with the experimental data with known parameters in the target values of each parameter. The target error is the threshold error value. The comparison is made for the first iteration which reaches the threshold value. The optimisation routine is continued to further evaluate the stability of the optimisation process. When available, the first iteration which crosses the error threshold is taken in the comparison tables. In the second part, a comparison is made between the accuracy over the different regression techniques for the most efficient optimisation routine in section 4.2. The initial guess is chosen fixed for all optimisation routines with random values: $Pulse_{start} = 0.8 sec$, (convective) Heat transfer coefficient = 10 (W/m^{2}K) and Thermal conductivity = 0.5 (W/m·K). All calculations are performed with an Intel®Core^{TM} i7-3930K CPU @ 3.20 GHz with 32 GB RAM.

4.1. Optimisation solver comparison

Piecewise polynomial regression. In contrast to what we expect from the knowledge of structural dynamics updating, we notice that the regression model built with a polynomial regression model does not properly converge for all optimisation routines. It is clearly seen in Table 3 and Figure 5 that the polynomial regression cannot optimise parameters with different influence degrees properly. The least influential parameter (Heat transfer coefficient) remains fixed until the two other parameters converge. Afterwards, the optimisation routine holds these two parameters stable and optimises the second parameter. This is shown in Figure 5 by the instantaneous error increase above 1000 calculation seconds. The reason for this behaviour is the approximation of the regression model which does not fit accurately the known FE simulation points in the regression model. It can also be seen that the Simplex method starts to oscillate close after the algorithm changes to optimise only the second parameter. Within these steps, the regression model encounters large local changes to finer estimate the global minimum. The Genetic algorithm has

12

Table 3: Comparison algorithms with Piecewise polynomial regression.

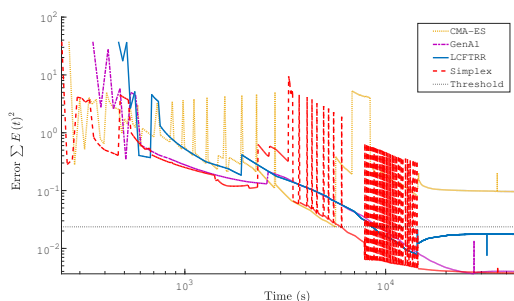| Description	Target	LCFTRR	Simplex	CMA-ES	GenAl
Pulse start time (s)	1.000	9.798e-1	1.022e-1	8.508e-1	9.796e-1
Heat transfer coefficient (W/m^{2}K)	8.5	1.1e1	1.1e1	1.1e1	1.1e1
Thermal conductivity (W/m·K)	9.630e-1	9.104e-1	9.244e-1	9.211e-1	9.105e-1
Iterations	/	270	331	293	271
Error $\sum E(t)^2$	2.360e-2	2.352e-2	2.345e-2	2.356e-2	2.343e-2
Time (s)	/	8.541e3	5.962e3	5.625e3	9.226e3

Figure 5: Comparison of all optimisation routines with the use of a piecewise polynomial regression.
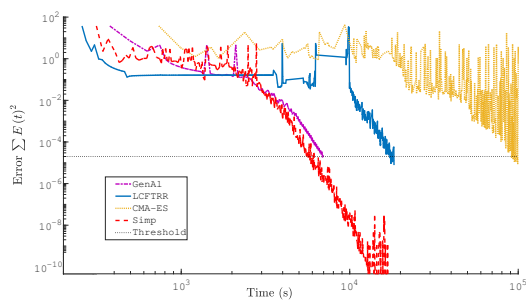

Figure 6: Comparison of all optimisation routines with the use of a scattered linear interpolation regression.

far fewer oscillations as this technique has a superior global approach character. As a threshold value to compare the different optimisation solvers, a stopping criterion of $\sum E(t)^2 = 2.360e - 2$ is used.

N-dimensional scattered linear interpolation. By comparing the different optimisation routines with a linear interpolation regression as shown in Table 4, one sees that there is an exceptional approximation possible. One of the major reasons is the exact fit through the FE points within the regression. When we compare the different optimisers against each other, we clearly notice that the approximation of the first and the third parameter are closer than the second due to the unequal importance of the parameters within the investigated temperature interval, but it can be seen that even the second parameter is estimated precisely. It is shown in Figure 6 that the Simplex and GenAl optimisations give the fastest results. It should be remarked that the Genetic algorithm needs the lowest number of iterations, accordingly the least amount of FE simulations, but the iteration time is over ten times larger than the iteration time of the Simplex method due to the larger amount of iterations used inside the genetic algorithm to find the minimum in the regression model. For this particular case this results in the best performance of the Simplex method due to the relatively simple FE model, but for more time-consuming FE models the Genetic algorithm will deliver faster results. In Figure 6 can also be seen that the CMA-ES largely oscillates before it starts to converge. As a threshold value to compare the different optimisation solvers, a stopping criterion of $\sum E(t)^2 = 2.000e - 5$ is used.

Table 4: Comparison algorithms with n-dimensional scattered linear interpolation.

Description	Target	LCFTRR	Simplex	CMA-ES	GenAl
Pulse start time (s)	1.000	1.000	9.996e-1	9.994e-1	9.998e-1
Heat transfer coefficient (W/m^{2}K)	8.5	8.4	8.4	8.4	8.4
Thermal conductivity (W/m·K)	9.630e-1	9.624e-1	9.626e-1	9.626e-1	9.622e-1
Iterations	/	511	260	399	120
Error $\sum E\left(t\right)^2$	2.000e-5	1.770e-5	1.732e-5	1.712e-5	1.812e-5
Time (s)	/	1.737e4	5.667e3	9.140e4	6.893e3

Table 5: Comparison algorithms with n-dimensional spline based regression

Description	Target	LCFTRR	Simplex	CMA-ES	GenAl
Pulse start time (s)	1.000	1.014	1.000	9.758e-1	1.015
Heat transfer coefficient (W/m^{2}K)	8.5	7.6	6.6	8.0	8.8
Thermal conductivity (W/m·K)	9.630e-1	9.711e-1	9.730e-1	9.623e-1	9.675e-1
Iterations	/	668	152	208	68
Error $\sum E\left(t\right)^2$	4.000e-3	3.707e-3	3.239e-3	5.751e-3	2.543e-3
Time (s)	/	9.598e2	7.316e2	3.168e3	3.413e3

N-dimensional spline regression. By comparing the optimisers for the n-dimensional spline regression, we receive similar results as with the linear interpolation, as shown in Table 5. There are a few differences we need to remark: First of all the global accuracy is almost ten times less than for the linear interpolation with the same amount of iterations. Secondly, the time used to converge is approximately ten times smaller than with the linear interpolation. This results mainly in a less accurate estimation of the second parameter, but in a faster global result. Only the Genetic algorithm has an equal distributed error between the three different parameters. Thereby is shown that the Genetic algorithm parameter estimation is relatively independent of the influence of the parameter, which makes it an interesting optimisation routine for white box estimation of unbalanced parameters in FEMU. Similar to the linear interpolation regression it is shown in Figure 7 and Table 5 that the Simplex method delivers the fastest results, but the Genetic algorithm delivers superior results for all parameters in fewer iterations which will make it interesting to use for more time-consuming FE simulations. Besides, Figure 7 also shows that the Genetic algorithm delivers the precisest results before one of its termination criteria are achieved. It needs to be remarked that the termination criteria are set equal for all compared optimisation routines. As a threshold value to compare the different optimisation solvers, a stopping criterion of $\sum E\left(t\right)^2 = 4.000e-3$ is used.

4.2. Response surface approximation comparison

The results of the different regression techniques are compared with respect to an equal accuracy in Table 6. As out of the three previous paragraphs can be concluded that for this test
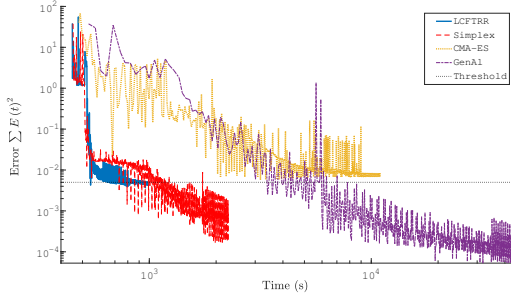
Figure 7: Comparison of all optimisation routines with a spline regression.
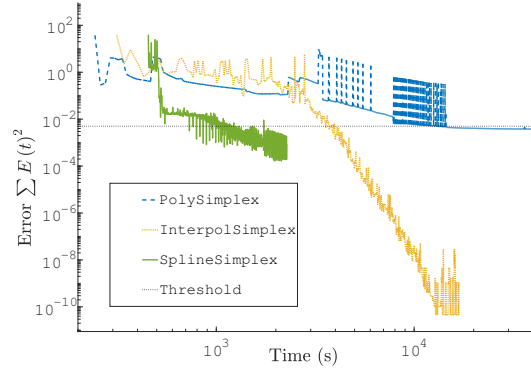

Figure 8: Comparison of all regression techniques using the Simplex optimisation routine.

Table 6: Comparison regression types to an error threshold of 4.000e-3 for the Simplex optimiser.

Description	Polynomial	Interpolation	Spline
Pulse start time (s)	1.011	9.955e-1	1.000
Heat transfer coefficient (W/m^{2}K)	8.5	7.0	6.6
Thermal conductivity (W/m·K)	9.516e-1	9.567e-1	9.730e-1
Iterations	1239	174	152
Error $\sum E\left(t\right)^2$	3.998e-3	3.714e-3	3.239e-3
Time (s)	2.197e4	3.733e3	7.316e2

case the Simplex method delivers the best results independent of the used regression technique. Figure 8 shows that due to the non-perfect fit through the FE simulation points, the polynomial regression delivers the least accurate results. We can even conclude that an exact fit through the FE simulation points within the regression model is a mandatory constraint for updating of thermal problems for NDE applications. The choice between interpolation and spline regression is complex as both of them have advantages. Spline regression delivers faster results until a certain accuracy in contrast to linear interpolation which solves longer but delivers stable and accurate improvements. This is shown in Figure 9 where the results of Figure 8 are plotted versus the iteration number instead of time. As a threshold value to compare the different response surface approximations, a stopping criterion of $\sum E\left(t\right)^2 = 4.000e-3$ is used.

4.3. Sensitivity analysis

The sensitivity analysis based on the FAST method initiated by Cukier et al [63] is shown in Table 7. It can be seen that globally there are no significant differences between the different regression models and optimisation solvers. The sensitivities to the different parameters are different with a major influence of parameter 1 in contrast to the two other parameters, as already explained in section 3.1. The only remark are the combination of the interpolation regression with the Genetic algorithm and the least square optimisation solver for the first parameter. A clear
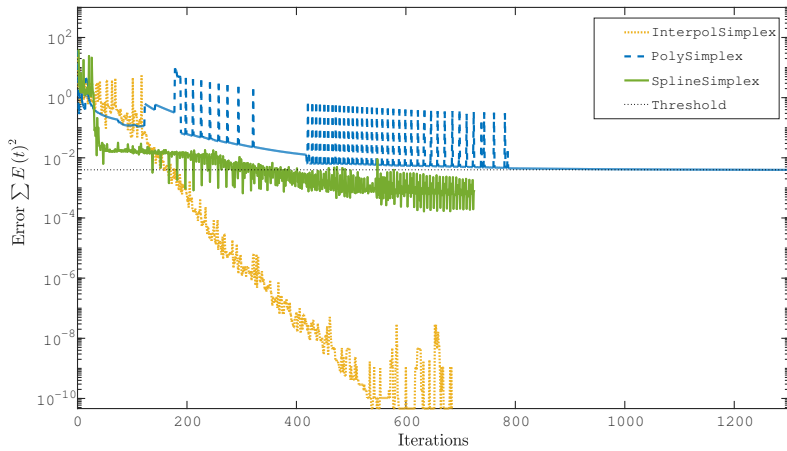
Figure 9: Comparison of all regression techniques for the Simplex optimiser plotted versus iteration number.

explanation could not be found for it. Perhaps, this is the result of an initial parameter choice which is close to the target value. Thereby the influence of the parameter is lower due to a flat propagation of the response function for this parameter.

Conclusions

In this work, we demonstrated that the implementation of well-known FEMU routines when applied to a physically varying problem results in varying performances. The implementation in thermal NDE applications requires an exact fit through the known FE output values in the regression stage to successfully estimate the different parameters in a non-linear problem. Additionally, an overview is presented of the different possible optimisation routines and their predictive abilities of thermal NDE model updating. To summarise the results, it is shown that the Simplex method in combination with a spline regression performs ideal for less computation intensive FE models. However, the Genetic algorithm in combination with a linear interpolation regression model performs better for complex FE models. The results of this work can be used to choose the broadest applicable combination of optimisation routine and regression model for FE model updating of multiphysics problems and deliver an extra added value to the state of the art of model updating in structural dynamics. The presented results open perspectives for a broader usage of model updating, for example, to improve the probability of defect detection in active thermography or efficiency improvement in sequential inspection routines.

Acknowledgements

16

Table 7: Sensitivity analysis of the different optimisation routines and regression models in correspondence with the work of Cannavo [62].

Description	Pulse param	h param	κ param
Interpolation CMAES	0.2070	0.0219	0.0214
Interpolation GenAl	0.0612	0.0279	0.0330
Interpolation LCFTRR	0.0697	0.0478	0.0456
Interpolation Simplex	0.1640	0.0439	0.0302
Polynomial CMAES	0.1538	0.0289	0.0263
Polynomial GenAl	0.1206	0.0659	0.0473
Polynomial LCFTRR	0.1800	0.0697	0.0475
Polynomial Simplex	0.1086	0.0308	0.0345
Spline CMAES	0.2301	0.0583	0.0407
Spline GenAl	0.2099	0.0546	0.0252
Spline LCFTRR	0.1790	0.0351	0.0405
Spline Simplex	0.2139	0.0328	0.0326

Bibliography

[1] K. M. Abd El-Ghany, M. M. Farag, Expert system to automate the finite element analysis for non-destructive testing, NDT and E International 33 (6) (2000) 409–415. doi:10.1016/S0963-8695(00)00009-8.

[2] D. Foti, M. Diaferio, N. I. Giannoccaro, M. Mongelli, Ambient vibration testing, dynamic identification and model updating of a historic tower, NDT & E International 47 (2012) 88–95. doi:10.1016/j.ndteint.2011.11.009.
URL http://dx.doi.org/10.1016/j.ndteint.2011.11.009

[3] M. Meo, G. Zumpano, Damage assessment on plate-like structures using a global-local optimization approach, Optimization and Engineering 9 (2) (2008) 161–177. doi:10.1007/s11081-007-9016-0.

[4] J. Mottershead, M. Friswell, Model Updating In Structural Dynamics: A Survey (1993). doi:10.1006/jsvi.1993.1340.
URL http://www.sciencedirect.com/science/article/pii/S0022460X83713404

[5] G. Steenackers, P. Guillaume, Finite element model updating taking into account the uncertainty on the modal parameters estimates, Journal of Sound and Vibration 296 (4-5) (2006) 919–934. doi:10.1016/j.jsv.2006.03.023.
URL http://linkinghub.elsevier.com/retrieve/pii/S0022460X06002719

[6] H.-C. Cheng, Y.-H. Tsai, K.-N. Chen, J. Fang, Thermal placement optimization of multichip modules using a sequential metamodeling-based optimization approach, Applied Thermal Engineering 30 (17-18) (2010) 2632–2642. doi:10.1016/j.applthermaleng.2010.07.004.
URL http://linkinghub.elsevier.com/retrieve/pii/S1359431110002875

[7] V. Isakov, Inverse Problems for Partial Differential Equations, 2nd Edition, Vol. 127 of Applied Mathematical Sciences, Springer-Verlag, New York, 2006. doi:10.1007/0-387-32183-7.
URL http://link.springer.com/10.1007/0-387-32183-7

[8] P. Chaudhuri, P. Santra, S. Yoele, A. Prakash, D. Reddy, L. Lachhvani, J. Govindarajan, Y. Saxena, Non-destructive evaluation of brazed joints between cooling tube and heat sink by IR thermography and its verification using FE analysis, NDT & E International 39 (2) (2006) 88–95. doi:10.1016/j.ndteint.2005.08.002.
URL http://linkinghub.elsevier.com/retrieve/pii/S0963869505001167

[9] M. Louaayou, N. Naït-Saïd, F. Z. Louai, 2D finite element method study of the stimulation induction heating in synchronic thermography NDT, NDT & E International 41 (8) (2008) 577–581. doi:10.1016/j.ndteint.2008.07.001.
URL http://linkinghub.elsevier.com/retrieve/pii/S096386950800073X

[10] F. Mabrouki, M. Genest, G. Shi, a. Fahr, Numerical modeling for thermographic inspection of fiber metal laminates, NDT and E International 42 (7) (2009) 581–588. doi:10.1016/j.ndteint.2009.02.010.
URL http://dx.doi.org/10.1016/j.ndteint.2009.02.010

[11] S. Sfarra, C. Ibarra-Castanedo, F. Lambiase, D. Paoletti, a. Di Ilio, X. Maldague, From the experimental simulation to integrated non-destructive analysis by means of optical and infrared techniques: results compared, Measurement Science and Technology 23 (11) (2012) 115601. doi:10.1088/0957-0233/23/11/115601.
URL   http://stacks.iop.org/0957-0233/23/i=11/a=115601?key=crossref.c8fe083c180a09d96da550526c744d47

[12] R. K. Nagle, E. B. Saff, A. D. Snider, Fundamentals of Differential Equations and Boundary Value Problems, Pearson education, 2012.

[13] M. Vollmer, K. Möllmann, Infrared thermal imaging: fundamentals, research and applications, Wiley-VCH, Berlin, 2010.
URL   http://books.google.com/books?hl=en{\&}lr={\&}id=5SSiZAMwxtYC{\&}oi=fnd{\&}pg=PR15{\&}dq=Infrared+thermal+imaging:+fundamentals,+research+and+applications{\&}ots=ClTOKRc2sH{\&}sig=oRgWvTf06VZj2g0iXLoElTWHaxs

[14] M. Susa, C. Ibarra-Castanedo, Pulse thermography applied on a complex structure sample: comparison and analysis of numerical and experimental results, in: IV Conferencia Panamer-

icana de END Buenos Aires, 2007, p. 12.
URL http://212.8.206.21/article/panndt2007/papers/54.pdf

[15] S. Lau, D. Almond, J. Milne, A quantitative analysis of pulsed video thermography, NDT & E International 24 (4) (1991) 195–202. doi:10.1016/0963-8695(91)90267-7.
URL http://linkinghub.elsevier.com/retrieve/pii/0963869591902677

[16] C. Ibarra-Castanedo, M. Genest, J.-M. Piau, S. Guibert, A. Bendada, X. P. V. Maldague, Active Infrared Thermography Techniques for the Non-destructive Testing of Materials, in: Ultrasonic and Advanced Methods for Nondestructive Testing and Material Characterization, Chen, CH, 2007, pp. 325–348.
URL http://medcontent.metapress.com/index/A65RM03P4874243N.pdf

[17] G. Steenackers, F. Presezniak, P. Guillaume, Development of an adaptive response surface method for optimization of computation-intensive models, Computers & Industrial Engineering 57 (3) (2009) 847–855. doi:10.1016/j.cie.2009.02.016.
URL http://linkinghub.elsevier.com/retrieve/pii/S0360835209000825

[18] T. Marwala, Finite-element-model Updating Using Computational Intelligence Techniques, Springer, 2010.
URL http://books.google.com/books?id=ObtwUF1uAqMC{\&}pgis=1

[19] J. Peeters, G. Arroud, B. Ribbens, J. Dirckx, G. Steenackers, Updating a finite element model to the real experimental setup by thermographic measurements and adaptive regression optimization, Mechanical Systems and Signal Processing 64-65 (2015) 428–440. doi:10.1016/j.ymssp.2015.04.010.
URL http://linkinghub.elsevier.com/retrieve/pii/S0888327015001697

[20] W. I. Thacker, J. Zhang, L. T. Watson, J. B. Birch, M. A. Iyer, M. W. Berry, Algorithm 905: SHEPPACK: Modified Shepard Algorithm for Interpolation of Scattered Multivariate Data, ACM Trans. Math. Softw. 37 (3) (2010) 34:1—-34:20. doi:10.1145/1824801.1824812.

[21] S. Hosder, L. T. Watson, B. Grossman, W. H. Mason, H. Kim, R. T. Haftka, S. E. Cox, Polynomial Response Surface Approximations for the Multidisciplinary Design Optimization of a High Speed Civil Transport, Optimization and Engineering 2 (4) (2001) 431–452.

[22] A. Azadeh, S. F. Ghaderi, M. Sheikhalishahi, B. P. Nokhandan, Optimization of Short Load Forecasting in Electricity Market of Iran Using Artificial Neural Networks, Optimization and Engineering (2014) 485–508doi:10.1007/s11081-012-9200-8.
URL http://www.springerlink.com/index/10.1007/s11081-012-9200-8

[23] M. T. Hagan, M. B. Menhaj, Training Feedforward Networks with the Marquardt Algorithm, IEEE Transactions on Neural Networks 5 (6) (1994) 989–993. doi:10.1109/72.329697.

[24] P. Dashora, G. Gupta, J. Dashora, Thermal conductivity, diffusivity and heat capacity of plasticized polyvinyl chloride, Indian Journal of Pure and applied Physics 43 (February)

(2005) 132–136.
URL `http://nopr.niscair.res.in/handle/123456789/8720`

[25] (Xenics Vision), Sensor-Gobi384-1471 (2010).

[26] (Xenics Vision), D. Uwaerts, Gobi Interface Control Document XP Gobi 384-1471 (2008).

[27] X. Maldague, F. Galmiche, A. Ziadi, Advances in pulsed phase thermography, Infrared physics & technology 1 (418) (2002) 1–11.
URL `http://www.sciencedirect.com/science/article/pii/S135044950200138X`

[28] J. Peeters, G. Steenackers, B. Ribbens, G. Arroud, J. Dirckx, Finite element optimization by pulsed thermography with adaptive response surfaces, in: Proceedings of the 2014 International Conference on Quantitative InfraRed Thermography, University of Antwerp, QIRT Council, Bordeaux, 2014, p. 10. doi:10.21611/qirt.2014.039.
URL `http://qirt.org/archives/qirt2014doi/papers/QIRT-2014-039.pdf`

[29] X. Maldague, S. Marinetti, Pulse phase infrared thermography, Journal of Applied Physics 79 (5) (1996) 2694. doi:10.1063/1.362662.
URL `http://link.aip.org/link/JAPIAU/v79/i5/p2694/s1{\&}Agg=doi`

[30] P. Brown, A. Hindmarsh, L. Petzold, Using Krylov Methods in the Solution of Large-Scale Differential-Algebraic Systems, SIAM Journal Scientific Computing 15 (1994) 1467–1488.

[31] (Comsol Multiphysics), Comsol Documentation (2015).

[32] A. J. Chapman, Heat transfer, 4th Edition, Macmillan, New York, 1984.

[33] R. L. Thomas, J. J. Pouch, Y. H. Wong, L. D. Favro, P. K. Kuo, A. Rosencwaig, Subsurface flaw detection in metals by photoacoustic microscopya, Journal of Applied Physics 51 (2) (1980) 1152–1156.

[34] C. Ibarra-Castanedo, X. P. V. Maldague, Interactive methodology for optimized defect characterization by quantitative pulsed phase thermography, Research in Nondestructive Evaluation 16 (4) (2005) 175–193. doi:10.1080/09349840500351846.

[35] G. Busse, Optoacoustic phase angle measurement for probing a metal, Applied Physics Letters 35 (10) (1979) 759–760.

[36] A. Rosencwaig, G. Busse, High-resolution photoacoustic thermal-wave microscopy, Applied Physics Letters 36 (9) (1980) 725–727.

[37] J. Peeters, B. Ribbens, J. J. J. Dirckx, G. Steenackers, Determining directional emissivity : Numerical estimation and experimental validation by using infrared thermography, Infrared Physics & Technologydoi:10.1016/j.infrared.2016.06.016.

[38] T. L. Bergman, A. S. Lavine, F. P. Incropera, D. P. DeWitt, Fundamentals of Heat and Mass Transfer, 7th Edition, John Wiley & Sons, Incorporated, 2011.

[39] A. Darabi, X. Maldague, Neural network based defect detection and depth estimation in TNDE, NDT & E International 35 (3) (2002) 165–175.
URL `http://ac.els-cdn.com/S096386950100041X/1-s2.0-S096386950100041X-main.pdf?{\_}tid=48a5f622-9d30-11e3-b900-00000aacb360{\&}acdnat=1393231825{\_}c8c438208474ca17a066479cb5d67f35http://www.sciencedirect.com/science/article/pii/S096386950100041X`

[40] Granta Design Limited, CES Edupack 2013 (2013).

[41] (professional thermographers association), Emissivity Values for Common Materials (2014).
URL `http://www.infrared-thermography.com/material.htm`

[42] G. Gary Wang, Z. Dong, P. Aitchison, Adaptive Response Surface Method - a Global Optimization Scheme for Approximation-Based Design Problems, Engineering Optimization 33 (6) (2001) 707–733. doi:10.1080/03052150108940940.

[43] X. S. Nguyen, A. Sellier, F. Duprat, G. Pons, Adaptive response surface method based on a double weighted regression technique, Probabilistic Engineering Mechanics 24 (2) (2009) 135–143. doi:10.1016/j.probengmech.2008.04.001.
URL `http://dx.doi.org/10.1016/j.probengmech.2008.04.001`

[44] A. Iwasaki, A. Todoroki, T. Sugiya, Remote Smart Damage Detection via Internet with Unsupervised Statistical Diagnosis, Springer Netherlands, Dordrecht, 2003, pp. 157–166.
URL `http://dx.doi.org/10.1007/978-94-017-0371-0{\_}16`

[45] L. Faravelli, S. Casciati, Structural damage detection and localization by response change diagnosis, Progress in Structural Engineering and Materials 6 (2) (2004) 104–115. doi:10.1002/pse.171.
URL `http://doi.wiley.com/10.1002/pse.171`

[46] S. E. Fang, R. Perera, A response surface methodology based damage identification technique, Smart Materials and Structures 18 (6) (2009) 065009. doi:10.1088/0964-1726/18/6/065009.

[47] W.-X. Ren, H.-B. Chen, Finite element model updating in structural dynamics by using the response surface method, Engineering Structures 32 (8) (2010) 2455–2465. doi:10.1016/j.engstruct.2010.04.019.
URL `http://dx.doi.org/10.1016/j.engstruct.2010.04.019`

[48] C. Kim, S. Wang, K. K. Choi, Efficient Response Surface Modeling by Using Moving Least-Squares Method and Sensitivity, AIAA Journal 43 (11) (2005) 2404–2411.

[49] G. Jekabsons, ARESLab Adaptive Regression Splines toolbox for Matlab / Octave (2011).
URL `http://www.cs.rtu.lv/jekabsons/`

21

[50] P. Alfeld, Scattered data interpolation in three or more variables, Mathematical Methods in Computer Aided Geometric Design (1989) 1–33.
URL `http://citeseerx.ist.psu.edu/viewdoc/download?doi=10.1.1.35.2949{\&}rep=rep1{\&}type=pdf{\%}5Cnpapers://d4024fd7-a3f3-42d0-af66-5e8b9b0d2151/Paper/p7013`

[51] (MathWorks), The Matlab user manual (2017).

[52] T. Coleman, Y. Li, An interior trust region approach for nonlinear minimization subject to bounds, SIAM Journal on optimization.
URL `http://epubs.siam.org/doi/abs/10.1137/0806023`

[53] D. Marquardt, An algorithm for least-squares estimation of nonlinear parameters, Journal of the Society for Industrial & Applied ... 151 (3712) (1963) 859–60. doi:10.1126/science.151.3712.859-b.
URL `http://www.ncbi.nlm.nih.gov/pubmed/17746741http://epubs.siam.org/doi/pdf/10.1137/0111030`

[54] J. Nocedal, S. J. Wright, Numerical Optimization, Springer Series in Operations Research and Financial Engineering, Springer-Verlag, New York, 1999. doi:10.1007/b98874.
URL `http://link.springer.com/10.1007/b98874`

[55] C. Offord, Ž. Bajzer, A Hybrid Global Optimization Algorithm Involving Simplex and Inductive Search, in: Computational Science - ICCS 2001, Vol. 2074, Springer, 2001, pp. 680–688.
URL `http://link.springer.com/10.1007/3-540-45718-6{\_}73`

[56] Z. Bajzer, I. Penzar, Strategic Simplex algorithm (1999).

[57] C. Igel, N. Hansen, S. Roth, Covariance matrix adaptation for multi-objective optimization., Evolutionary computation 15 (1) (2007) 1–28. doi:10.1162/evco.2007.15.1.1.

[58] N. Hansen, S. Kern, Evaluating the CMA Evolution Strategy on Multimodal Test Functions., in: 8th International Conference on Parallel Problem Solving from Nature PPSN VIII, Springer, 2004, pp. 282–291.

[59] R. Levin, N. Lieven, Dynamic finite element model updating using simulated annealing and genetic algorithms, Mechanical Systems and Signal Processing 12 (1998) 1195–1201.
URL `http://www.sciencedirect.com/science/article/pii/S0888327096901363`

[60] R. Perera, A. Ruiz, C. Manzano, Performance assessment of multicriteria damage identification genetic algorithms, Computers and Structures 87 (1-2) (2009) 120–127. doi:10.1016/j.compstruc.2008.07.003.
URL `http://dx.doi.org/10.1016/j.compstruc.2008.07.003`

[61] Z. Tu, Y. Lu, FE model updating using artificial boundary conditions with genetic algorithms, Computers & Structures 86 (7-8) (2008) 714–727. doi:10.1016/j.compstruc.2007.07.005.

[62] F. Cannavó, Sensitivity analysis for volcanic source modeling quality assessment and model selection, Computers & Geosciences 44 (2012) 52–59. doi:10.1016/j.cageo.2012.03.008.

[63] R. I. Cukier, C. M. Fortuin, K. E. Shuler, A. G. Petschek, J. H. Schaibly, Study of the sensitivity of coupled reaction systems to uncertainties in rate coefficients. I Theory, Journal of Chemical Physics 59 (8) (1973) 3873–3878. doi:10.1063/1.1680571.